

# ALDH1L2 drives HCC progression through TAM polarization

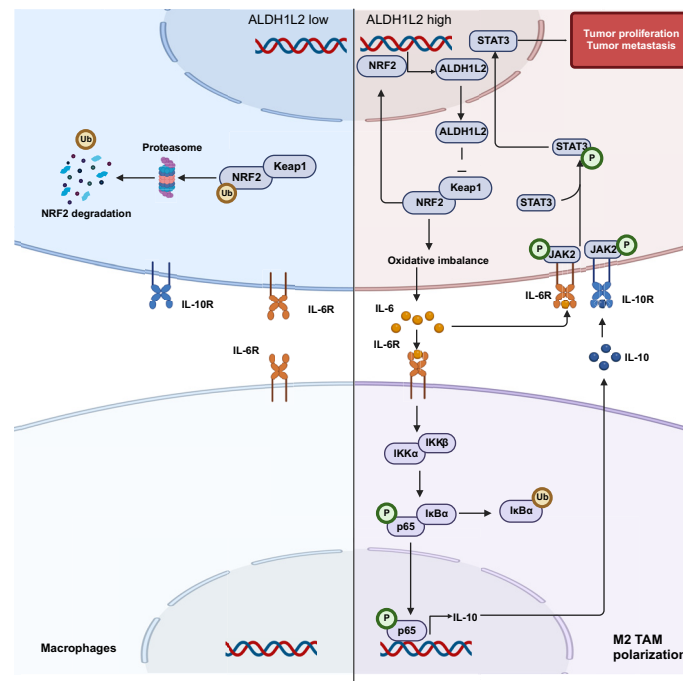
## Authors

Jiajun Li, Chi Zhang, Qingqing Zhou, ..., Xi-Dai Long, Jun Wu, Hua Tian

## Correspondence

[sjtulongxd@263.net](mailto:sjtulongxd@263.net) (X.-D. Long), [jun.wu@shsmu.edu.cn](mailto:jun.wu@shsmu.edu.cn) (J. Wu), [htian@shsci.org](mailto:htian@shsci.org) (H. Tian).

## Graphical abstract



## Highlights:

- ALDH1L2 promotes HCC cell proliferation, migration, invasion, and metastasis.
- Elevated ALDH1L2 expression is associated with poor prognosis in HCC.
- ALDH1L2 promotes HCC progression by activating the IL-6/Jak2/STAT3 signaling axis and promoting TAM polarization.
- ALDH1L2 knockdown sensitizes HCC cells to sorafenib.

## Impact and implications:

This research highlights that ALDH1L2 could serve as a predictive and prognostic marker in HCC. We found that a positive feedback loop between ALDH1L2 and NRF2 promotes HCC progression by activating the IL-6/Jak2/STAT3 signaling axis and tumor-associated macrophage polarization. In addition, we found that ALDH1L2 knockdown enhances the anti-HCC effect of sorafenib.

# ALDH1L2 drives HCC progression through TAM polarization

Jiajun Li<sup>1,†</sup>, Chi Zhang<sup>1,†</sup>, Qingqing Zhou<sup>1,†</sup>, Qinqin Long<sup>2,3,†</sup>, Jiayi Chen<sup>4,†</sup>, Lili Meng<sup>5,†</sup>, Wei Tian<sup>1</sup>, Yue Yang<sup>1</sup>, Chao Ge<sup>1</sup>, Yuting Su<sup>1</sup>, Xi-Dai Long<sup>2,3,\*</sup>, Jun Wu<sup>4,\*</sup>, Hua Tian<sup>1,2,3,\*</sup>

JHEP Reports 2025. vol. 7 | 1–15



**Background & Aims:** Dysregulation of one-carbon metabolism is considered an early hallmark of mitochondrial dysfunction and cancer metabolism. ALDH1L2 belongs to the aldehyde dehydrogenase family and plays an important role in tumor progression. However, little is known about the precise role and underlying mechanisms of ALDH1L2 in hepatocellular carcinoma (HCC).

**Methods:** Immunohistochemistry, western blotting, and immunofluorescence staining were used to evaluate ALDH1L2 expression in HCC samples (n = 90) and cell lines (n = 9). A series of *in vitro* and *in vivo* assays were performed to explore the role and molecular mechanism of ALDH1L2 in HCC progression.

**Results:** ALDH1L2 upregulation is associated with poor prognosis in HCC (hazard ratio 1.923; 95% confidence interval 1.03–3.59;  $p = 0.04$ ). ALDH1L2 promotes tumor cell proliferation and metastasis by activating NRF2/IL-6/STAT3 signaling. ALDH1L2 promotes mitochondrial respiration, increases ATP production and protects HCC cells from reactive oxygen species-induced cellular damage via NRF2 stabilization. NRF2 also directly binds to the ALDH1L2 promoter and increases ALDH1L2 transcription, thereby establishing a positive feedback loop to maintain the function of ALDH1L2. The interaction between tumor-associated macrophages and ALDH1L2-overexpressing HCC cells further promotes HCC progression. In addition, ALDH1L2 knockdown enhances the anti-HCC activity of the tyrosine kinase inhibitor sorafenib.

**Conclusions:** These findings provide the first evidence indicating that ALDH1L2 is directly involved in tumor progression by interacting with tumor-associated macrophages through the Jak2/STAT3 signaling pathway and that ALDH1L2 may be a target molecule for HCC therapy.

© 2024 The Author(s). Published by Elsevier B.V. on behalf of European Association for the Study of the Liver (EASL). This is an open access article under the CC BY-NC-ND license (<http://creativecommons.org/licenses/by-nc-nd/4.0/>).

## Introduction

Hepatocellular carcinoma (HCC) is the most common type of liver cancer and the third leading cause of cancer-related death worldwide.<sup>1</sup> Although great progress has been made in research on HCC in the past few decades, HCC still has a poor prognosis, mainly because of metastasis, recurrence, and drug resistance [49]. However, the exact mechanisms of tumor occurrence and metastasis remain largely unclear. Thus, the identification of potential regulatory genes involved in HCC may reveal therapeutic targets to improve the prognosis of HCC.

One-carbon metabolism includes the folate and methionine cycles and supports cellular requirements for growth and proliferation. Dysregulation of one-carbon metabolism is an early hallmark of mitochondrial dysfunction and cancer metabolism.<sup>2,3</sup> Accumulating evidence suggests that one-carbon metabolism is critical for cancer development. One-carbon metabolic enzymes are important targets for cancer treatment. Limitations in the supply of one-carbon units may have therapeutic benefits for

cancer patients. Antifolates are among the oldest antimetabolite classes of anticancer agents and were one of the first modern anticancer drugs.<sup>4</sup> Methotrexate is used as an essential component of current chemotherapeutic regimens that exhibit substantial efficacy in the treatment of numerous malignancies.<sup>5</sup> However, these drugs have many deleterious side effects owing to the importance of tetrahydrofolate in healthy tissues. Therefore, the identification of new chemotherapeutic targets in folate metabolism is warranted. The desuccinylation of the mitochondrial serine hydroxymethyltransferase SHMT2 is a pivotal signal in cancer cells to reprogram serine metabolism to support rapid growth.<sup>6</sup> Phosphoglycerate dehydrogenase (PHGDH) is the major rate-limiting enzyme in the first step of the serine–glycine–one-carbon (SGOC) metabolic pathway.<sup>7</sup> Dysregulation of PHGDH influences serine synthesis and downstream one-carbon metabolism. The presence of PHGDH heterogeneity in primary tumors could be considered a marker for tumor aggressiveness.<sup>8</sup> PHGDH is a potential therapeutic target for the treatment of metastatic tumors<sup>9</sup> and targeting PHGDH is an effective approach to overcome tyrosine kinase inhibitor (TKI)

\* Corresponding authors. Addresses: State Key Laboratory of Systems Medicine for Cancer, Shanghai Cancer Institute, Renji Hospital, Shanghai Jiao Tong University School of Medicine, 25/Ln 2200, Xie-Tu Road, Shanghai 200032, China. Tel./Fax: +86-21-64436627 (H. Tian); Department of Laboratory Medicine, Shanghai General Hospital Jiading Branch, Shanghai Jiao Tong University School of Medicine, Shanghai 201803, China (J. Wu); Department of Pathology, The Affiliated Hospital of Youjiang Medical University for Nationalities, 533000 Baise, Guangxi, China (X.-D. Long).

E-mail addresses: [sjtulongxd@263.net](mailto:sjtulongxd@263.net) (X.-D. Long), [jun.wu@shsmu.edu.cn](mailto:jun.wu@shsmu.edu.cn) (J. Wu), [htian@shsci.org](mailto:htian@shsci.org) (H. Tian).

† These authors contributed equally.

<https://doi.org/10.1016/j.jhepr.2024.101217>



drug resistance in HCC.<sup>10</sup> Methylene tetrahydrofolate dehydrogenase 1 like plays an essential role in supporting HCC cell growth.<sup>11</sup> Methylene tetrahydrofolate dehydrogenase 2 contributes to the progression of renal cell carcinoma via a novel epitranscriptomic mechanism involving Hypoxia-inducible factor-2 $\alpha$ .<sup>12</sup> Understanding the importance of one-carbon metabolism in cancer cell growth is anticipated to lead to the development of more selectively inhibiting individual one-carbon pathway enzymes for cancer treatment and intervention.

Aldehyde dehydrogenase 1 family member L1 (ALDH1L1) and aldehyde dehydrogenase 1 family member L2 (ALDH1L2) are two key folate-metabolizing enzymes. ALDH1L1 is a cytosolic 10-formyltetrahydrofolate dehydrogenase, whereas ALDH1L2 is the mitochondrial homolog of 10-formyltetrahydrofolate dehydrogenase.<sup>13</sup> The biological roles of ALDH1L1 and ALDH1L2 are quite different although the two proteins share approximately 72% amino acid sequence identity and are close structural and enzymatic homologs.<sup>13,14</sup> ALDH1L1 inhibits tumor cell motility via dephosphorylation of cofilin by PP1 and PP2A in A549 cells.<sup>15</sup> Downregulation of ALDH1L1 expression is associated with poor prognosis in HCC.<sup>16</sup> ALDH1L1 knockout promotes liver tumor growth.<sup>17</sup> These results suggest that ALDH1L1 can function as a tumor suppressor. Previous studies have shown that high expression of ALDH1L2 is associated with poor prognosis in pancreatic ductal adenocarcinoma.<sup>18</sup> ALDH1L2 is upregulated in human colorectal tumor tissues compared with normal tissues.<sup>19</sup> Recent reports have shown that colorectal cancer patients with low ALDH1L2 expression exhibit radio-resistance.<sup>20</sup> Previous reports have shown that oxidative stress inhibits the distant metastasis of human melanoma cells. These reports also showed that ALDH1L2 was much more highly expressed in liver metastatic nodules than in subcutaneous tumors in both donor and recipient mice.<sup>21</sup> However, new research indicates that the loss of ALDH1L2 can support metastatic progression by promoting formate and formyl-methionine (fMet) production in breast cancer cells.<sup>22</sup> These results indicate that ALDH1L2 plays a cellular context-dependent role in different tumor types. However, evidence on the role and clinical significance of ALDH1L2 expression in HCC is limited. Thus, the function and molecular mechanism underlying the role of ALDH1L2 in HCC and the relationships between ALDH1L2 expression and clinicopathological parameters remain unclear. Here, we examined the potential role of ALDH1L2 in HCC progression and explored the mechanism by which ALDH1L2 affects HCC cell proliferation and metastasis.

## Materials and methods

Further information can be found in the [Supplementary material](#), Methods section.

The sequences of shRNA targets are listed in [Table S1](#).

The primer sequences are listed in [Table S2](#).

Information on the antibodies is provided in [Table S3](#).

### Mitochondrial oxygen consumption assay

The oxygen consumption rate (OCR) was evaluated with a Mito Stress Test Kit (Agilent, Cat. No. 103015-100, California, CA, USA) as described previously.<sup>23</sup> Mitochondrial respiration

inhibitors (oligomycin, FCCP, and antimycin A + rotenone) were used to treat the cells in the assay system.

### Orthotopic and subcutaneous tumor model models and treatment

For the *in vivo* xenograft experiment, a microsyringe was used to orthotopically inoculate nude mice in the left hepatic lobe through an 8-mm transverse incision made in the upper abdomen under anesthesia[48]. A total of  $2 \times 10^6$  HCC cells suspended in 40  $\mu$ l of a mixture of serum-free DMEM/Matrigel (1:1 volume) (BD Biosciences, MA, USA) were inoculated into each male nude mouse.

For the *in vivo* isograft experiment, male C57BL/6J mice were subcutaneously injected with  $5 \times 10^6$  Hepa1-6 derived cells. After 24 days, the mice were sacrificed.

For *in vivo* drug studies, 6-week-old male BALB/c nude mice were injected subcutaneously with  $2 \times 10^6$  cells. When the tumor volume was approximately 100 mm<sup>3</sup>, the mice were randomized into four groups. The mice were treated with sorafenib (10 mg/kg, once every other day) via intraperitoneal injection. The tumor dimensions were measured with a Vernier calipers every 3 days, and the tumor volume was calculated as follows: tumor volume = (length  $\times$  width<sup>2</sup>)/2.

Four or six weeks later, the mice were sacrificed, and the tumors along with the liver and lung tissues from individual mice were excised and fixed with 4% phosphate-buffered neutral formalin for at least 72 h. Metastatic tissues were analyzed via H&E staining. All animal experiments were approved by the Laboratory Animal Ethics Committee of Renji Hospital, Shanghai Jiao Tong University School of Medicine (approval number: RT2022-122u).

### Statistical analysis

All data are shown as the mean  $\pm$  standard deviation (SD) values and were analyzed with IBM SPSS Statistics 21 (IBM, Chicago, IL, USA). Graphs were generated with GraphPad Prism 7.0 (GraphPad Software, San Diego, CA, USA). Statistical comparisons of the data were performed via two-tailed Student *t* tests or via one-way ANOVA for multiple comparisons among more than two groups. Overall survival curves were generated via the Kaplan–Meier method and compared via the log-rank test. Univariate and multivariate analyses were performed with a stepwise Cox proportional hazard regression model. A value of  $p < 0.05$  was considered to indicate statistical significance (\* $p < 0.05$ , \*\* $p < 0.01$ ).

## Results

### ALDH1L2 is a marker of poor prognosis in HCC patients

ALDH1L2 expression was upregulated in HCC tissues compared with noncancerous tissues according to analysis of The Cancer Genome Atlas (TCGA) and Gene Expression Omnibus (GEO) datasets and the ICGC-LIRI-JP cohort (Fig. 1A–E). These results were also confirmed by western blotting (WB) and immunohistochemistry (IHC) staining (Fig. 1F and G). Furthermore, in the TCGA dataset, ALDH1L2 expression was upregulated in patients with nodal metastasis compared with patients without nodal metastasis (Fig. 1H). In addition, ALDH1L2 upregulation was confirmed to be related to

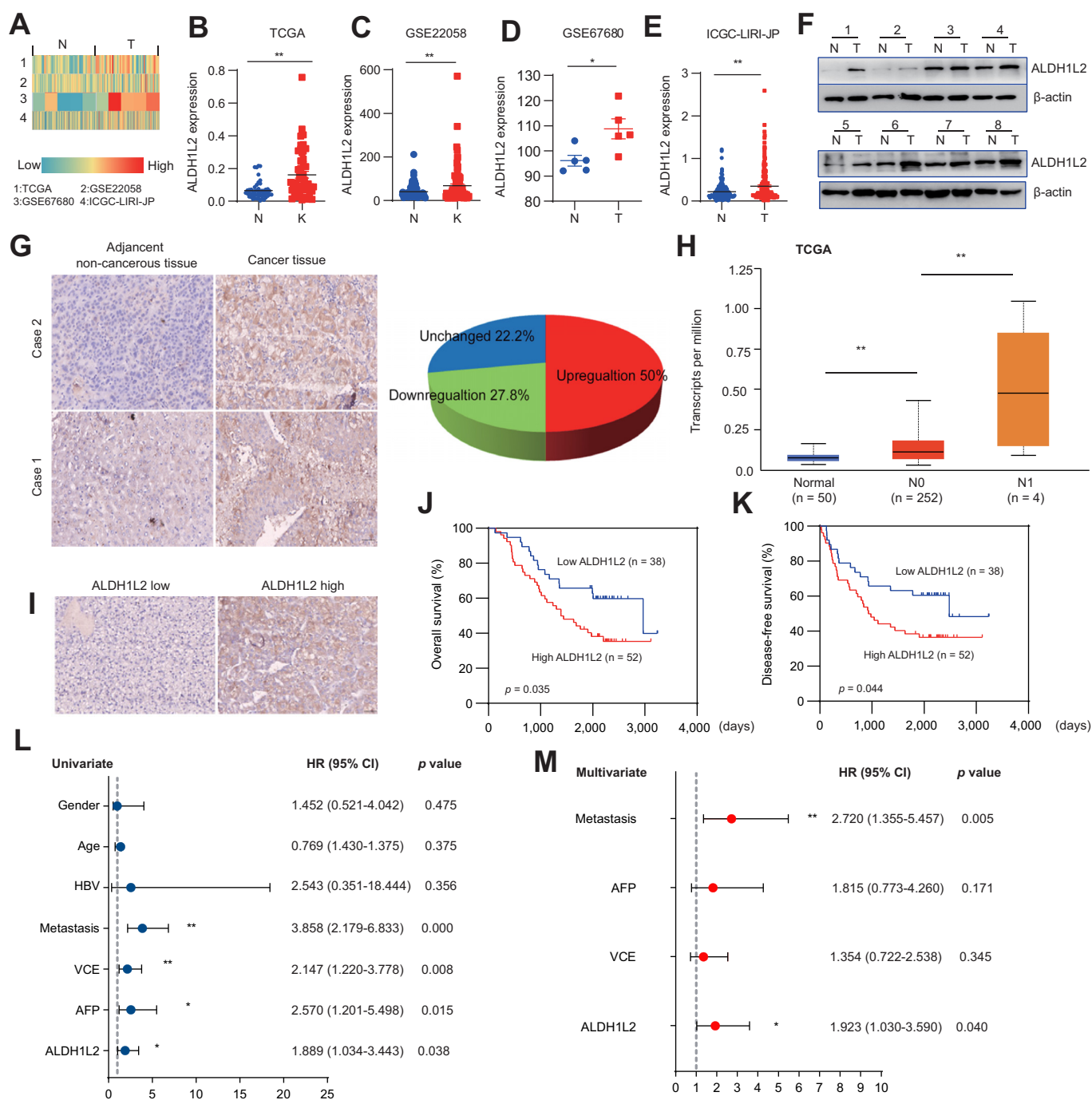


**Fig. 1. ALDH1L2 upregulation is associated with poor prognosis in HCC.** (A) Heatmap showing ALDH1L2 expression in the TCGA dataset, GEO dataset and ICGC-LIRI-JP cohorts. (B–E) ALDH1L2 expression in HCC tissues was compared with that in the corresponding noncancerous liver tissues in the TCGA dataset (n = 50) (B), GSE22058 dataset (C), GSE67680 dataset (D), and ICGC-LIRI-JP cohort (E). (F) ALDH1L2 expression in HCC tissues was compared with that in the corresponding noncancerous liver tissues via Western blotting. (G) Immunohistochemical analysis of ALDH1L2 expression in HCC samples and corresponding noncancerous liver tissues. Representative images are shown. (H) ALDH1L2 expression in noncancerous liver tissues, HCC tissues and metastatic cancer tissues was analyzed via TCGA data. (I) Representative images of cells with high and low ALDH1L2 expression. (J,K) OS and DFS of patients with HCC stratified by the ALDH1L2 expression level, Log-rank test. (L,M) Univariate and multivariate Cox proportional hazards regression analyses were conducted to evaluate the effect of ALDH1L2 on overall survival in patients with HCC. Data are represented as mean ± SD. \**p* <0.05; \*\**p* <0.01. Unpaired t-test. DFS, disease-free survival; GEO, Gene Expression Omnibus; HCC, hepatocellular carcinoma; OS, overall survival; TCGA, The Cancer Genome Atlas; ICGC-LIRI-JP, International Cancer Genome Consortium liver cancer-RIKEN Japan.

tumor metastasis in datasets for other solid cancers from the TCGA (Fig. S1A) and GEO datasets (Fig. S2).

The clinicopathological features of HCC patients (n = 90) are shown in Table S4. On the basis of the IHC results, the

patients were divided into two groups on the basis of ALDH1L2 expression in the tumor tissue (Fig. 1I). ALDH1L2 expression was positively associated with TNM stage and capsule invasion status. However, there were no correlations

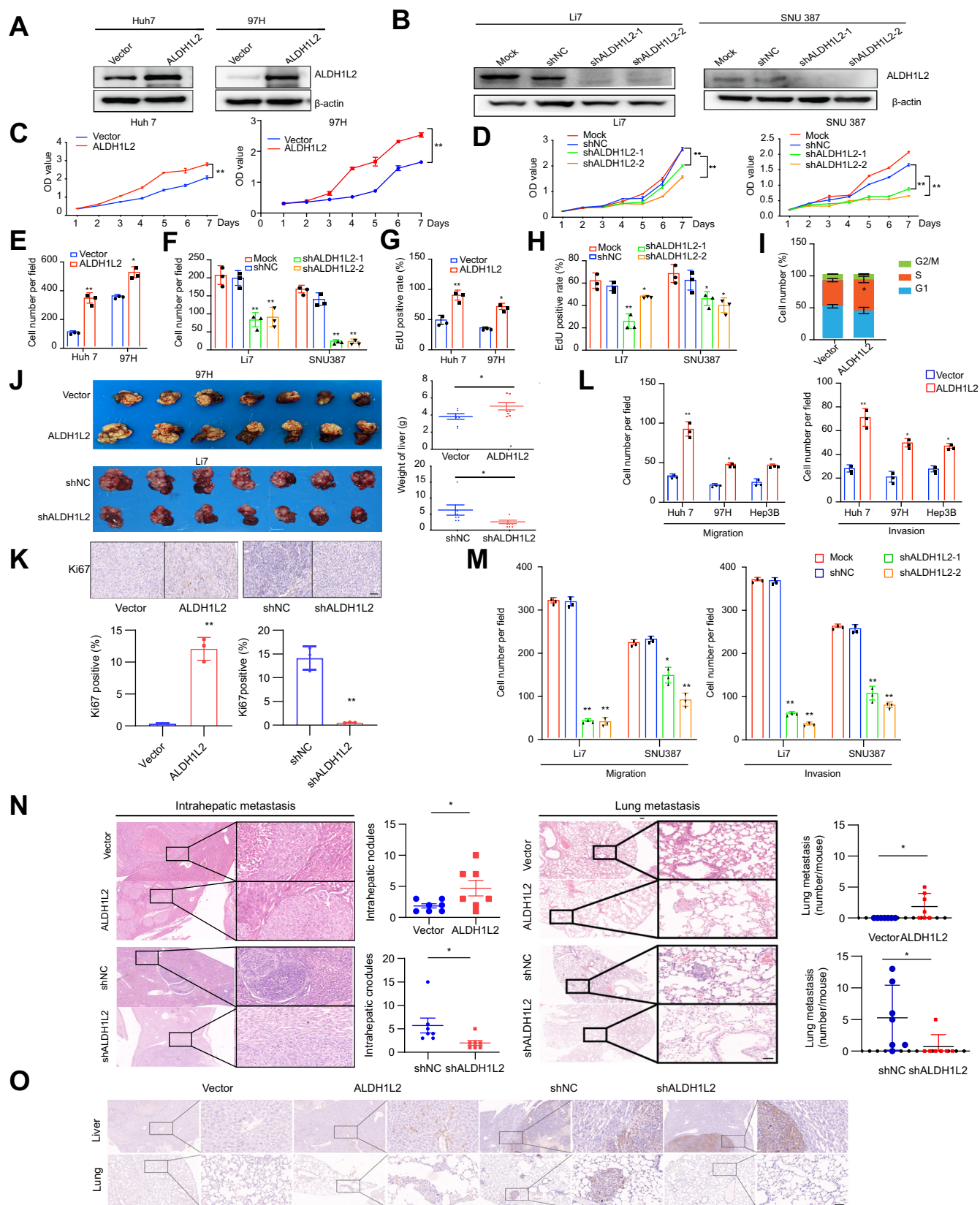


**Fig. 2. ALDH1L2 increases HCC cell proliferation, invasion and metastasis.** The expression level of ALDH1L2 was measured by Western blotting in ALDH1L2-overexpressing (A) and ALDH1L2-knockdown (B) HCC cells. Cell proliferation was assessed by a CCK8 assay (C,D), a colony formation assay (E,F) and an EdU incorporation assay (G,H). (I) The cell cycle distribution of ALDH1L2-overexpressing Huh7 cells was analyzed by flow cytometry. (J) Liver tissues from animals bearing xenografts derived from MHCC-97H cells with stable ALDH1L2 overexpression or from Li7 cells with stable ALDH1L2 knockdown. The dot plots show the results of the

between ALDH1L2 expression and other clinicopathological factors, such as sex, age, tumor grade, cirrhosis status, serum alpha-fetoprotein level, portal vein tumor thrombus, vessel carcinoma embolus, tumor size, and HBV positivity status (Table S5). We next evaluated the prognostic value of ALDH1L2 in HCC. Survival analysis of the HCC patients based on the IHC staining results was performed, and the results indicated that patients with higher ALDH1L2 expression had markedly worse overall survival (OS;  $p = 0.035$ ) and disease-free survival (DFS;  $p = 0.044$ ) than patients with lower ALDH1L2 expression (Fig. 1J and K). Furthermore, univariate and multivariate Cox proportional hazard analyses suggested that higher expression of ALDH1L2 was more strongly associated with worse survival in HCC patients than low ALDH1L2 expression in HCC patients ( $p < 0.05$ ; Fig. 1L and M). In addition, high expression of ALDH1L2 was associated with shorter OS times in patients with various types of tumors according to analysis of TCGA data (Fig. 1B). Thus, these findings suggested that ALDH1L2 could be a valuable prognostic factor for survival in patients with HCC.

#### ALDH1L2 promotes HCC cell growth *in vitro* and *in vivo*

On the basis of the endogenous expression of ALDH1L2 in HCC cell lines, the Huh7, MHCC-97H, Hep3B, SNU387, and Li7 cell lines were selected for gain- and loss-of-function studies (Fig. S3). Overexpression of ALDH1L2 increased the proliferation of HCC cells, whereas knockdown of ALDH1L2 decreased the proliferation of HCC cells (Fig. 2A–H, Fig. S4). Overexpression of ALDH1L2 promoted the G1/S transition in Huh7 cells (Fig. 2I, Fig. S5).

In the *in vivo* mouse xenograft model, overexpression of ALDH1L2 increased HCC tumor growth, whereas knockdown of ALDH1L2 decreased HCC tumor growth (Fig. 2J). Furthermore, Ki67 expression was higher in ALDH1L2-overexpressing tumor tissues and lower in ALDH1L2-knockdown tumor tissues (Fig. 2K). Therefore, these results show that ALDH1L2 promotes HCC cell proliferation.

#### ALDH1L2 promotes HCC cell invasion and metastasis

Overexpression of ALDH1L2 dramatically increased cell migration and invasion, whereas knockdown of ALDH1L2 had the opposite effect (Fig. 2L and M, Fig. S6). Matrix metalloproteinases (MMPs) are proteolytic enzymes that play major roles in tumor invasion. We found that the expression of MMP9 and MMP2 was upregulated in ALDH1L2-overexpressing cells and downregulated in ALDH1L2-knockdown cells (Fig. S7).

We next investigated the effect of ALDH1L2 on HCC metastasis *in vivo*. Histological examination of lung and liver tissues revealed that more numbers of intrahepatic metastatic nodules and lung metastases in mice bearing tumors derived

from ALDH1L2-overexpressing cells than in mice bearing tumors derived from control cells, with the opposite pattern found for ALDH1L2 knockdown (Fig. 2N). To further confirm metastasis, we used a human-specific antimitochondrial antibody to confirm the human origin of the cells and found more positively stained regions in the tumors derived from ALDH1L2-overexpressing cells. In contrast, compared with tumors derived from shNC control cells, tumors derived from ALDH1L2-knockdown cells exhibited a regular boundary and fewer positively stained regions (Fig. 2O). Taken together, these findings suggest that ALDH1L2 promotes HCC metastasis.

#### ALDH1L2 is critical for maintaining mitochondrial-associated metabolism in HCC cells

Cellular NADPH is essential for maintaining redox homeostasis and maintaining reductive biosynthesis, which are indispensable for tumorigenesis and cancer progression.<sup>24</sup> Furthermore, the results of the TCGA analysis revealed that the expression of ALDH1L2 was associated with the activity of the reactive oxygen species (ROS) pathway in multiple tumor types including HCC (Fig. S8). The colocalization of ALDH1L2 with a mitochondrial indicator (pDsRed1-Mito) was also detected in HCC cells (Fig. S9). Therefore, we examined the effects of ALDH1L2 on the NADPH/NADP<sup>+</sup> ratio and intracellular ROS levels. Overexpression of ALDH1L2 decreased intracellular ROS levels and increased the intracellular NADPH/NADP<sup>+</sup> ratio in HCC cells, whereas ALDH1L2 knockdown had the opposite effects (Fig. 3A–D, Fig. S10). Furthermore, we found that the overexpression of ALDH1L2 suppressed H<sub>2</sub>O<sub>2</sub>-induced ROS generation in HCC cells, whereas ALDH1L2 knockdown had the opposite effect (Fig. 3E and F). Collectively, these data indicate that ALDH1L2 is critical for maintaining the NADPH levels for redox homeostasis and thereby supports HCC cell proliferation.

As mitochondria are a major source of ROS, we next examined ROS levels in mitochondria via MitoSOX Red staining. The mitochondrial superoxide anion level was significantly higher in ALDH1L2-knockdown cells than in the corresponding control cells (Fig. 3G). As the mitochondrial membrane potential (mtMP) is a key indicator of mitochondrial activity, we examined the mtMP in ALDH1L2-knockdown HCC cells via a JC-1 assay. Our results showed that the mtMP in ALDH1L2-knockdown cells was lower than that in the corresponding control cells (Fig. 3H).

To determine whether the knockdown of ALDH1L2 affects mitochondrial respiration, we next evaluated the OCR, ATP production, and maximal respiratory capacity. The results revealed that the knockdown of ALDH1L2 reduced basal cellular respiration, decreased the intracellular ATP levels, and reduced the spare respiratory capacity and the mitochondrial OCR (Fig. 3I–M). Therefore, these results indicate that

quantitative analysis of liver weight. (K) Ki67 expression in xenografts derived from MHCC-97H ALDH1L2-overexpressing or Li7-shALDH1L2 cells and the corresponding control vector-transduced cells was evaluated via IHC staining. (L,M) The effects of ALDH1L2 overexpression (L) and knockdown (M) on HCC cell migration and invasion were assessed via Transwell assays. (N) Representative images of intrahepatic nodules and lung nodules formed by ALDH1L2-overexpressing MHCC-97H cells, ALDH1L2-knockdown Li7 cells and the corresponding control cells are shown. The numbers of intrahepatic metastatic nodules and lung metastatic nodules are shown in the right panel. (O) IHC analysis of metastasis with human-specific anti-mitochondria antibodies. Bar = 50  $\mu$ m. Data are represented as mean  $\pm$  SD. \* $p < 0.05$ ; \*\* $p < 0.01$ . Unpaired t-test or one-way ANOVA. CCK8, Cell Counting Kit-8; HCC, hepatocellular carcinoma; IHC, immunohistochemistry.

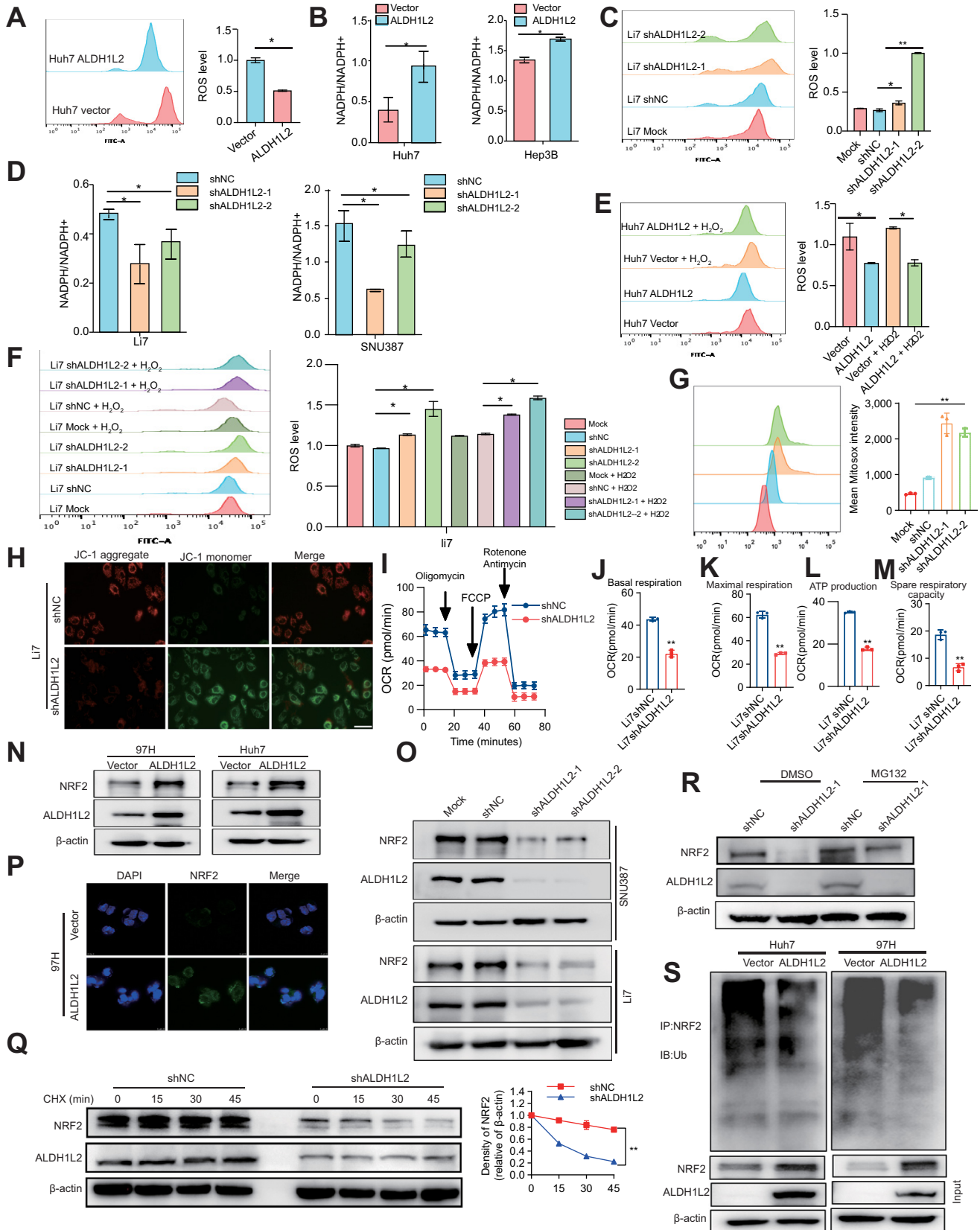


**Fig. 3. ALDH1L2 induces ROS accumulation via the regulation of NRF2 stability.** (A) The level of ROS in ALDH1L2-overexpressing and control cells was assessed by flow cytometry. (B) The intracellular NADPH/NADP<sup>+</sup> ratio was determined in ALDH1L2-overexpressing and control cells. (C) The level of ROS in ALDH1L2-knockdown cells was assessed via flow cytometry. (D) The intracellular NADPH/NADP<sup>+</sup> ratio was determined in ALDH1L2 knockdown cells. (E,F) The level of ROS was assessed by flow cytometry in ALDH1L2-overexpressing (E) and ALDH1L2-knockdown (F) cells treated with H<sub>2</sub>O<sub>2</sub>. (G) Mitochondrial ROS levels in cells stained

ALDH1L2 promotes cellular respiration and the generation of ATP and oxidative metabolites in tumor cells.

### ALDH1L2 increases the expression of nuclear factor E2-related factor 2 and prevents its degradation in HCC cells

As a leucine zipper transcription factor, nuclear factor E2-related factor 2 (NRF2) plays an important role in the maintenance of redox homeostasis.<sup>25</sup> We next explored the effect of ALDH1L2 on NRF2 expression in HCC cells. Overexpression of ALDH1L2 promoted NRF2 protein expression in HCC cells, whereas ALDH1L2 knockdown had the opposite effect (Fig. 3N and O). However, ALDH1L2 overexpression and knockdown did not affect NRF2 mRNA expression in HCC cells (Fig. S11). The results of the immunofluorescence assay revealed that the expression and nuclear translocation of NRF2 were increased in ALDH1L2-overexpressing HCC cells compared with vector-transduced cells (Fig. 3P, Fig. S12).

To confirm the influence of ALDH1L2 on NRF2 protein stability, we incubated ALDH1L2-knockdown and control HCC cells with cycloheximide (CHX) (50 µg/ml), which blocks *de novo* protein synthesis. In the presence of cycloheximide, knockdown of ALDH1L2 resulted in a higher rate of NRF2 degradation than detected in control cells, suggesting that the expression of the ALDH1L2 protein increases the stability of the NRF2 protein (Fig. 3Q). The half-life of the NRF2 protein in the cells decreased from 1 h to 15 min as a consequence of ALDH1L2 knockdown (Fig. 3Q). To investigate the involvement of the ubiquitin–proteasome pathway in the proteolytic degradation of NRF2, we treated ALDH1L2-knockdown HCC cells with MG132, a reversible proteasome inhibitor. Our results revealed that NRF2 degradation induced by ALDH1L2 knockdown was inhibited in the presence of MG132 (Fig. 3R). In addition, overexpression of ALDH1L2 resulted in decreased NRF2 ubiquitination (Fig. 3S). NRF2 expression is regulated primarily by Kelch-like ECH-associated protein 1 (KEAP1), a component of the Cullin 3 (CUL3)-based E3 ubiquitin ligase complex.<sup>26</sup> We found that the overexpression of ALDH1L2 suppressed KEAP1 expression, whereas the knockdown of ALDH1L2 had the opposite effect (Fig. S13A). To confirm the role of KEAP1 in the promoting effect of ALDH1L2 on NRF2 stability, we evaluated the expression of NRF2 in ALDH1L2-knockdown and ALDH1L2-overexpressing cells following the introduction of a KEAP1 overexpression plasmid or a KEAP1 shRNA. The ALDH1L2 overexpression-induced increase in NRF2 protein expression was reversed by the overexpression of KEAP1. Conversely, ALDH1L2 knockdown-induced decrease in NRF2 protein expression was reversed by the knockdown of KEAP1. Furthermore, ALDH1L2 attenuated NRF2 ubiquitination caused by overexpression of KEAP1 in

HCC cells (Fig. S13B and C). Collectively, these findings suggest that ALDH1L2 can stabilize NRF2 by directly preventing its ubiquitin–proteasome-mediated degradation.

### ALDH1L2 regulates HCC cell functions via the Jak2/STAT3 pathway

To explore the mechanism of ALDH1L2 in HCC, RNA-seq was performed in ALDH1L2-overexpressing cells. Kyoto Encyclopedia of Genes and Genome (KEGG) pathway enrichment analysis revealed that ALDH1L2 can regulate the Jak/signal transducer and activator of transcription 3 (STAT3) pathway in HCC cells (Fig. 4A). The IL-6/Jak/STAT3 signaling pathway was also enriched according to analysis of data obtained from the TCGA (Fig. S14). In addition, NRF2 has been reported to directly induce IL-6 transcription in hepatocytes.<sup>27</sup> Furthermore, ROS modulate various cellular signaling pathways, including the STAT3 pathway.<sup>28</sup> Therefore, we investigated the effects of ALDH1L2 on the IL-6/Jak/STAT3 pathway. Our results revealed that Jak2 but not Jak1 was activated in ALDH1L2-overexpressing HCC cells (Fig. 4B, Fig. S15A). The overexpression of ALDH1L2 increased the phosphorylation of STAT3, whereas ALDH1L2 knockdown had the opposite effect (Fig. 4B and C). Moreover, ALDH1L2 overexpression facilitated STAT3 nuclear entry in HCC cells (Fig. 4D, Fig. S15B). Furthermore, knockdown of ALDH1L2 inhibited the transcription of STAT3 target genes (Fig. S16).

Next, HCC cells were treated with a STAT3 inhibitor (BP-1-102) or transduced with STAT3 shRNA. The ALDH1L2 overexpression-induced increases in cell proliferation, migration, and invasion were reversed by treatment with BP-1-102 or STAT3 shRNAs (Fig. 4E–P, Fig. S15D–K). Furthermore, BP-1-102 suppressed STAT3 nuclear translocation in ALDH1L2-overexpressing HCC cells (Fig. 4F).

In addition, we found that the overexpression of ALDH1L2 upregulated IL-6 expression, whereas the knockdown of ALDH1L2 downregulated IL-6 expression in HCC cells (Fig. 5A). To confirm whether IL-6R participates in ALDH1L2-mediated activation of the Jak2/STAT3 pathway, ALDH1L2-overexpressing HCC cells were transduced with IL-6R shRNA. The increase in Jak2/STAT3 activity induced by ALDH1L2 overexpression was reversed by IL-6R shRNA transduction (Fig. S17). Therefore, these results suggest that ALDH1L2 regulates HCC cell functions by activating the IL-6/Jak2/STAT3 signaling pathway.

### ALDH1L2 promotes HCC progression by affecting tumor-associated macrophage polarization

The results of the gene ontology functional enrichment analysis revealed that ALDH1L2 can regulate the cytokine–cytokine

with MitoSOX Red were evaluated by flow cytometry. (H) The mtMP was assessed with the fluorescent mitochondrial probe JC-1. (I–M) The OCR was measured with a Seahorse XF24 Analyzer as detailed in the Materials and methods section (I). The basal mitochondrial respiration rate (J), maximal respiratory capacity (K), ATP production (L), and spare respiratory capacity (M) were calculated and statistically analyzed. (N,O) NRF2 expression in ALDH1L2-overexpressing (N) and ALDH1L2-knockdown (O) cells was measured by Western blotting. (P) NRF2 expression was evaluated by immunofluorescence staining. (Q) Stability of NRF2 in ALDH1L2-knockdown HCC cells treated with cycloheximide (CHX) at the indicated time points. (R) NRF2 expression in ALDH1L2-knockdown HCC cells treated with MG132 for 6 h. (S) Lysates of ALDH1L2-overexpressing and control HCC cells were subjected to immunoprecipitation with an anti-NRF2 antibody, and the immunocomplexes were analyzed by immunoblotting with an antibody specific for ubiquitin. Data are represented as mean ± SD. \**p* < 0.05; \*\**p* < 0.01. Unpaired t-test or one-way ANOVA. NRF2, nuclear factor E2-related factor 2; ROS, reactive oxygen species; OCR, oxygen consumption rate.



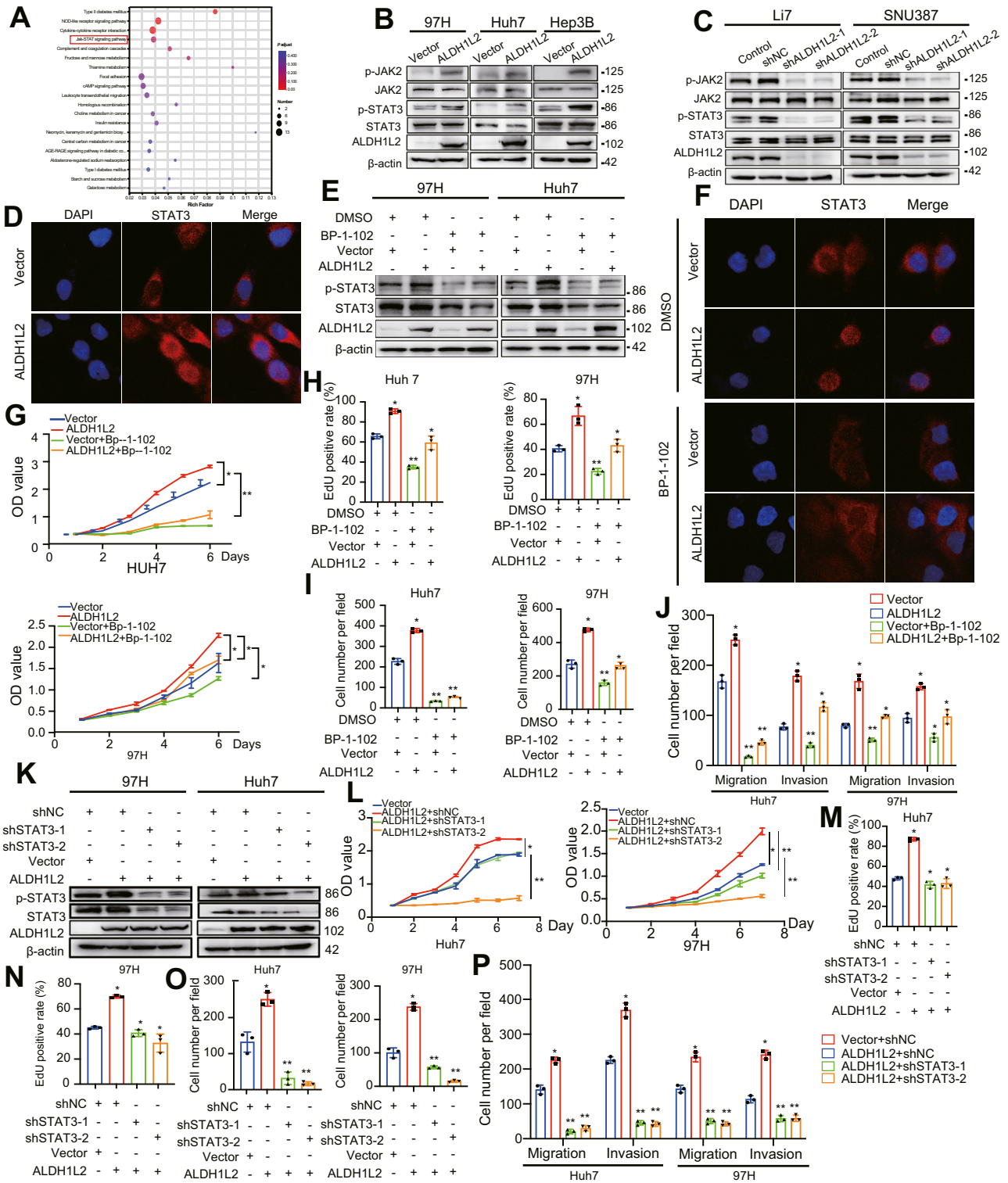
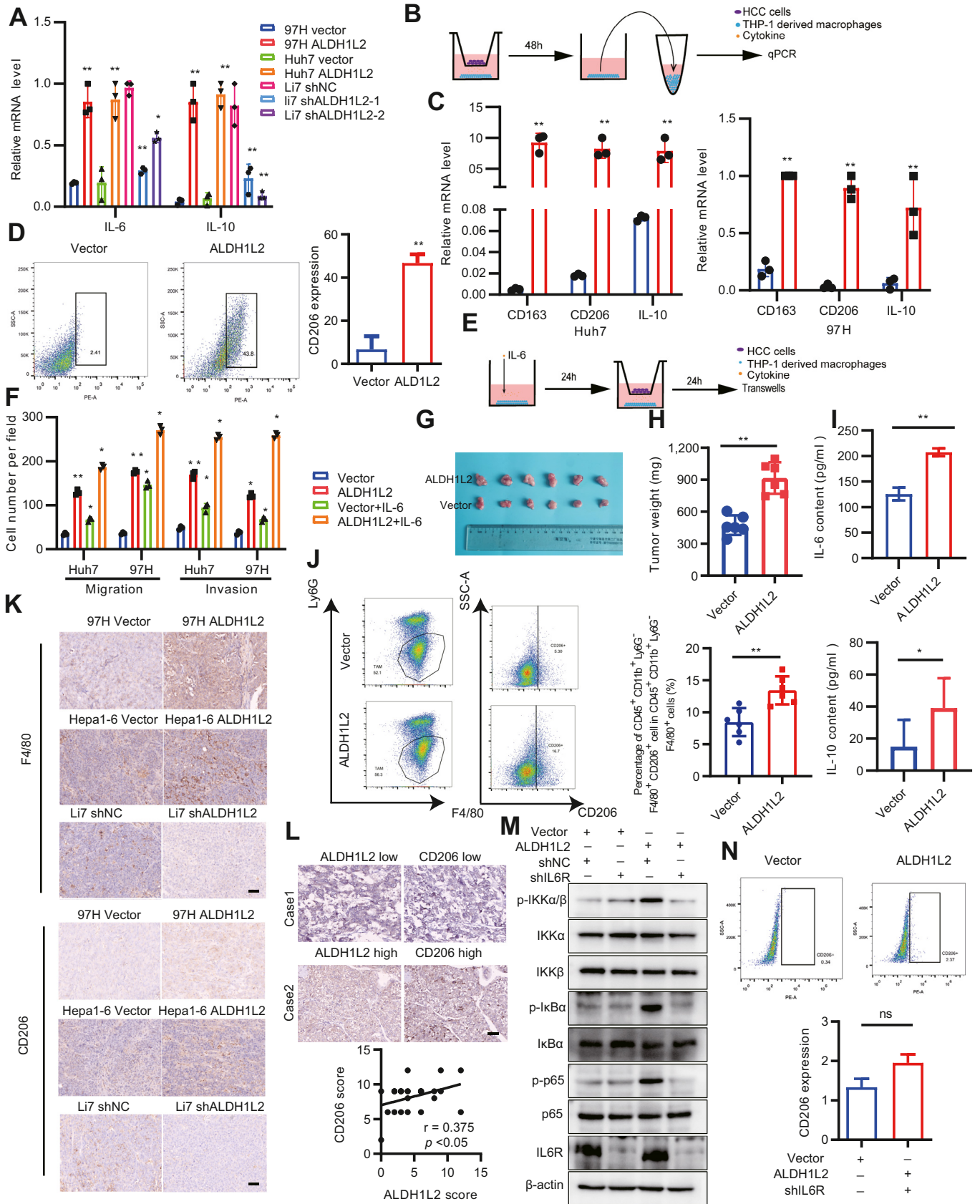


**Fig. 4. ALDH1L2 regulates HCC cell functions via the Jak2/STAT3 pathway.** (A) KEGG pathway analysis based on ALDH1L2 in HCC. (B,C) The protein levels of Jak2, p-Jak2, STAT3, and p-STAT3 in ALDH1L2-overexpressing (B) and ALDH1L2-knockdown (C) HCC cells were measured by Western blotting. (D) Effects of ALDH1L2 overexpression on the nuclear translocation of STAT3 as assessed by an immunofluorescence assay. (E,F) ALDH1L2-overexpressing HCC cells were treated with BP-1-102 or DMSO as indicated, and the level of STAT3 was measured by Western blotting (E) and evaluated by immunofluorescence staining (F). (G–J) ALDH1L2-overexpressing HCC cells were treated with BP-1-102 as indicated, and cell proliferation, migration and invasion were evaluated via a CCK8 assay (G), a colony formation assays (H), an EdU incorporation assay (I) and Transwell assays (J). (K) ALDH1L2-overexpressing HCC cells were transduced with STAT3 shRNA as indicated, and the level of STAT3 was measured by Western blotting. Cell proliferation, migration and invasion were evaluated via a CCK8 assay (L), an EdU incorporation assay (M,N), a colony formation assay (O), and Transwell assays (P). Data are represented as mean  $\pm$  SD. \* $p$  < 0.05; \*\* $p$  < 0.01. Unpaired t-test or one-way ANOVA. CCK8, Cell Counting Kit-8; HCC, hepatocellular carcinoma; KEGG, Kyoto Encyclopedia of Genes and Genome; STAT3, signal transducer and activator of transcription 3.



receptor interaction pathway in HCC cells (Fig. 4A). Moreover, we found that overexpression of ALDH1L2 increased the expression of IL-6 and IL-10, whereas ALDH1L2 knockdown had the opposite effect (Fig. 5A). Dysregulation of the inflammatory microenvironment can influence the crosstalk between cancer cells and components of the tumor microenvironment. Tumor-associated macrophages (TAMs) are important negative regulators of host innate immunity in the tumor microenvironment. IL-6 is recognized to be involved in alternative macrophage polarization.<sup>29,30</sup> To examine whether cancer cell invasion is affected by macrophages, coculture experiments with THP-1-derived macrophages were performed. The coculture experiments revealed upregulated expression of M2 polarization-related genes (CD163, CD206, and IL-10) in ALDH1L2-overexpressing cells (Fig. 5B–D). Furthermore, HCC cell migration and invasion were significantly increased in the presence of THP-1-derived macrophages pretreated with IL-6 (Fig. 5E–F).

To explore the role of TAMs in ALDH1L2-related HCC progression, ALDH1L2-overexpressing Hepa1-6 mouse HCC cells (Hepa1-6/ALDH1L2 cells) were transplanted into immunocompetent C57BL/6J mice. Overexpression of ALDH1L2 promoted tumor growth (Fig. 5G–H). Furthermore, overexpression of ALDH1L2 increased IL-6 and IL-10 secretion in C57BL/6J mice (Fig. 5I). Next, flow cytometry was used to evaluate TAM, myeloid-derived suppressor cell (MDSC), and regulatory T cell (Treg cell) infiltration in the harvested tumors. Implantation of Hepa1-6/ALDH1L2 cells significantly increased M2 TAM (marked by the CD45<sup>+</sup>/CD11b<sup>+</sup>/F4/80<sup>+</sup>/CD206<sup>+</sup>/Ly6G<sup>-</sup> signature) infiltration (Fig. 5J). Infiltration of MDSCs (marked by the CD45<sup>+</sup>/CD11b<sup>+</sup>/Ly6G<sup>+</sup> signature) and Treg cells (CD45<sup>+</sup>/CD4<sup>+</sup>/FOXP3<sup>+</sup>) was not observed (Fig. S18). Furthermore, IHC revealed that CD206-positive M2 macrophages were more abundant in tumors derived from ALDH1L2-overexpressing MHCC-97H cells but less abundant in tumors derived from ALDH1L2-knockdown Li7 cells than in tumors derived from the corresponding control cells (Fig. 5K). Moreover, ALDH1L2 expression is associated with the expression of M2 polarization-related genes (CD163, CD206, and IL-10) and M2 macrophage infiltration in many cancer types, including HCC, according to analysis of TCGA data (Figs S19–S21). Furthermore, IHC staining revealed a positive correlation between ALDH1L2 and CD206 expression in HCC (Fig. 5L). Therefore, these results demonstrate that ALDH1L2 impacts the recruitment and polarization of TAMs.

We next examined NF- $\kappa$ B expression in THP-1-derived macrophages. The results revealed that the NF- $\kappa$ B pathway

was activated in THP-1-derived macrophages treated with conditioned medium derived from ALDH1L2-overexpressing cells (Fig. 5M). IL-6R silencing was insufficient to promote NF- $\kappa$ B activation in THP-1-derived macrophages treated with conditioned medium derived from ALDH1L2-overexpressing cells (Fig. 5M). Furthermore, IL-6R silencing inhibited CD206 expression in THP-1-derived macrophages treated with conditioned medium from ALDH1L2-overexpressing cells (Fig. 5N).

M2-polarized TAMs secreted an increased amount of IL-10. The NF- $\kappa$ B p65 subunit can bind upstream of the IL10 gene and regulate the production of the IL-10 protein.<sup>31</sup> Furthermore, we found that IL-10 significantly promoted the migration and invasion of HCC cells as well as STAT3 activation in these cells. IL-10RA silencing reversed the effects of IL-10 on the activation of STAT3 in HCC cells (Fig. S22). Therefore, ALDH1L2 impacts the polarization of TAMs, which secrete IL-10 to mediate the activity of a positive feedback loop in HCC cells.

### NRF2 promotes the transcription of ALDH1L2 via a positive feedback loop

We found that the expression of ALDH1L2 was upregulated during H<sub>2</sub>O<sub>2</sub>-induced ROS generation in HCC cells (Fig. 6A, Fig. S23A). Sulforaphane (SFN) is an activator of NRF2. We found that SFN promoted ALDH1L2 expression in a dose- and time-dependent manner in HCC cells (Fig. 6B and C, Fig. S23B). Furthermore, knockdown of NRF2 suppressed ALDH1L2 expression in HCC cells (Fig. 6D and E). There are two putative antioxidant response elements (AREs) in the promoter of ALDH1L2 (-1,200 bp/+1 bp, Fig. 6F and G). Serial truncations of the ALDH1L2 promoter were generated on the basis of the location of the NRF2-binding sites (Fig. 6H). SFN was found to increase ALDH1L2 promoter activity (Fig. 6I). Knockdown of NRF2 inhibited ALDH1L2 promoter activity in HCC cells (Fig. 6J). The chromatin immunoprecipitation (ChIP) assay revealed that AREs (-280 to -270, -703 to -693) were immunoprecipitated with the anti-NRF2 antibody. However, the site with the strongest binding was site 1, which was closest to the transcription start site (Fig. 6K, Fig. S24). Furthermore, neither NRF2 knockdown nor SFN treatment regulated the activity of the ALDH1L2 promoter containing a putative NRF2-mutated binding site 1 (Fig. 6L, Fig. S25). Therefore, binding site 1 in the ALDH1L2 promoter is critical for NRF2 binding. Furthermore, we detected a significant positive correlation between the expression of ALDH1L2 and that of NRF2 in HCC

**Fig. 5. ALDH1L2 promotes HCC progression by affecting TAM polarization.** (A) The expression of IL-6 and IL-10 was analyzed via qRT-PCR in ALDH1L2-overexpressing and ALDH1L2-knockdown HCC cells. (B,C) After coculturing HCC cells (ALDH1L2-overexpressing or control cells) with THP-1-derived macrophages for 48 h, the relative mRNA levels of CD206 and CD163 in the macrophages were measured via qRT-PCR. Migration and invasion were assessed via Transwell assays. (D) CD206 expression was examined by flow cytometry. (E,F) THP-1-derived macrophages cells were pretreated with IL-6 for 24 h and were then cocultured with HCC cells in a Transwell apparatus for 48 h. Cell migration and invasion were examined via a Transwell assay. (G–K) Hepa1-6 cells stably transduced with ALDH1L2 or the corresponding control construct were subcutaneously injected into C57BL/6J mice. The dot plots show the results of the quantitative analysis of tumor weight (H). The concentrations of IL-6 and IL-10 in the serum of C57BL/6J mice were measured via ELISA (I). Flow cytometric analysis of the CD45<sup>+</sup>CD11b<sup>+</sup>Ly6G<sup>-</sup>F4/80<sup>+</sup>CD206<sup>+</sup>-M2 TAM population in tumor tissue (J). The expression of F4/80 and CD206 in xenograft and isograft mouse tumor tissues was evaluated via IHC staining (K). (L) The expression of CD206 and ALDH1L2 in HCC tissue was evaluated via IHC staining. The correlation between ALDH1L2 and CD206 expression in HCC tissues was analyzed. (M,N) After coculturing HCC cells (ALDH1L2-overexpressing or control cells) with THP-1-derived macrophages with or without IL-6R knockdown for 48 h, NF- $\kappa$ B protein expression was assessed via WB (M), and CD206 expression was examined via flow cytometry (N). Data are represented as mean  $\pm$  SD. \**p* < 0.05; \*\**p* < 0.01; ns, non-significant. Unpaired t-test or one-way ANOVA. HCC, hepatocellular carcinoma; IHC, immunohistochemistry; qRT-PCR, quantitative real-time-PCR; TAM, tumor-associated macrophage.

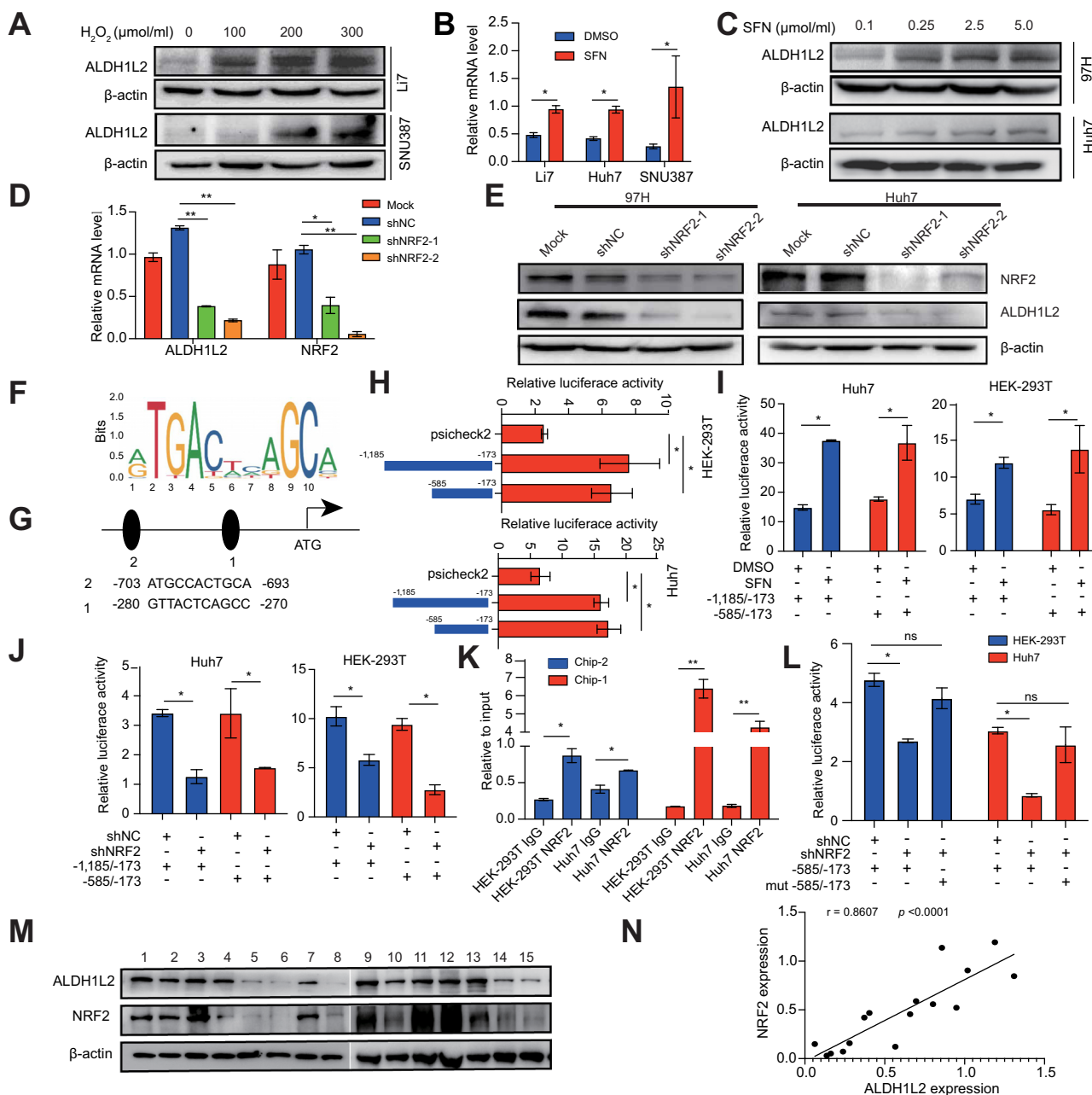


**Fig. 6. NRF2 binds to the ALDH1L2 promoter and increases ALDH1L2 expression.** (A) ALDH1L2 expression in HCC cells treated with H<sub>2</sub>O<sub>2</sub> was assessed via WB. (B–E) ALDH1L2 expression in HCC cells treated with SFN (B,C) and in NRF2-knockdown HCC cells (D–E) was measured via qRT-PCR and WB. (F,G) STAT3-binding motif. (H–J) Huh7 and HEK293T cells were transfected with different luciferase reporter vectors. The corresponding luciferase activities were measured via reporter gene assays (H). The cells were treated with SFN (I) or transfected with NRF2 shRNA or the control (J). The corresponding luciferase activities were measured via reporter gene assays. (K) ChIP followed by qRT-PCR analysis was performed to evaluate NRF2 binding to the ALDH1L2 promoter. (L) Huh7 and HEK293T cells were transfected with ALDH1L2 luciferase reporter vectors (containing wild-type or mutant NRF2-binding sites, -585/-173). The cells were transfected with an NRF2 shRNA vector or the corresponding control vector. The corresponding relative luciferase activities were determined via reporter gene assays. (M) ALDH1L2 and NRF2 expression in HCC tissues was measured via WB. (N) The correlation between ALDH1L2 and NRF2 expression in HCC tissues was analyzed (Spearman's correlation). Data are represented as mean ± SD. \**p* < 0.05; \*\**p* < 0.01. Unpaired t-test or one-way ANOVA. ChIP, chromatin immunoprecipitation; HCC, hepatocellular carcinoma; NRF2, nuclear factor E2-related factor 2; qRT-PCR, quantitative real-time-PCR; SFN, sulforaphane; STAT3, signal transducer and activator of transcription 3; WB, western blotting.

tissues (Fig. 6M and N). Similar results were obtained in many cancer types, including HCC via analysis of TCGA data (Fig. S26). Therefore, these results suggest that ALDH1L2/NRF2 can form a positive regulatory loop and promote HCC progression.

### Knockdown of ALDH1L2 sensitizes HCC cells to sorafenib treatment

Sorafenib is a first-line standard therapeutic agent for the treatment of advanced HCC. Sorafenib is a multikinase inhibitor

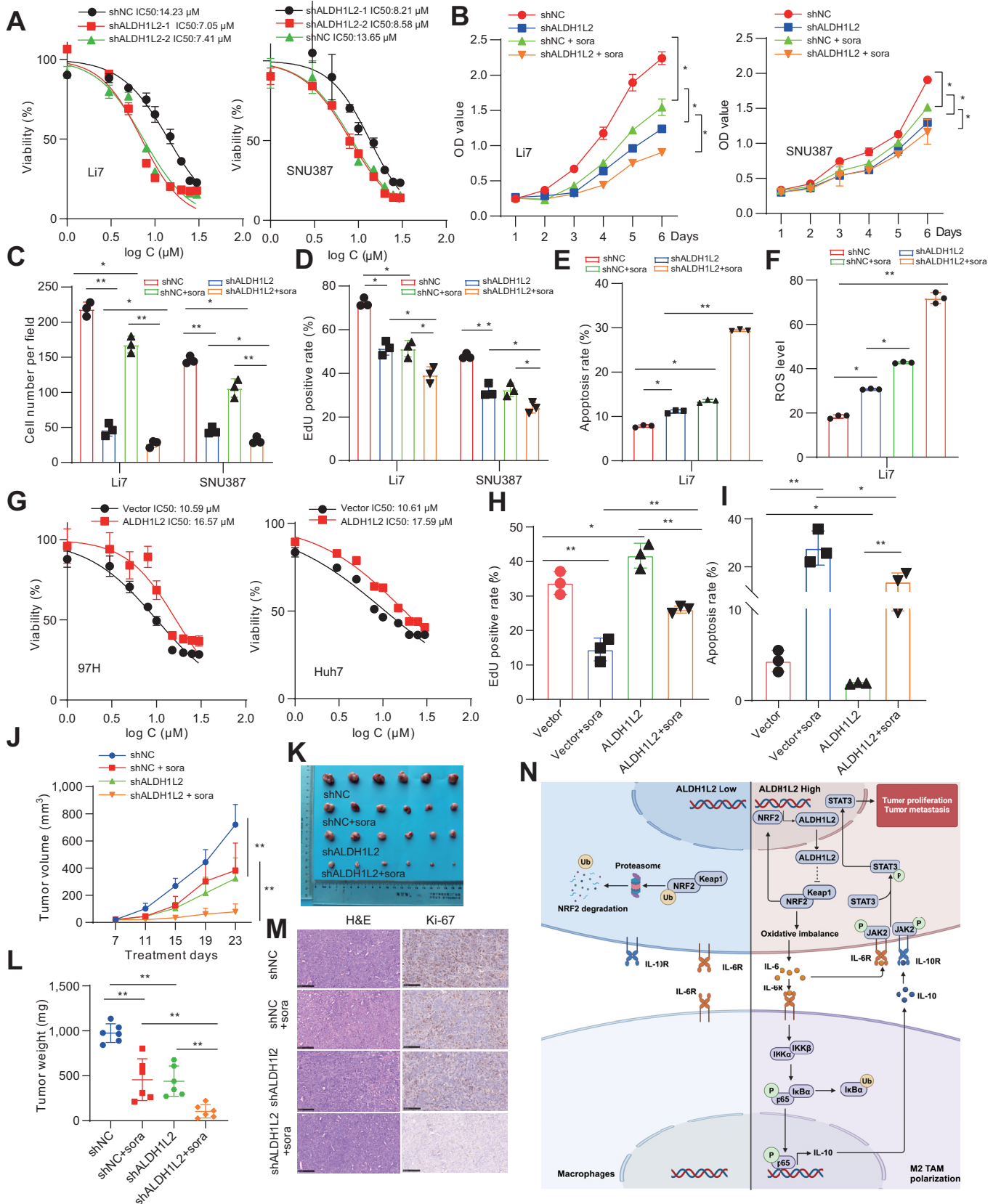


**Fig. 7. Knockdown of ALDH1L2 sensitizes HCC cells to sorafenib.** (A) The effect of ALDH1L2 knockdown on the IC50 of sorafenib in Li7 and SNU387 cells was evaluated. (B–F) ALDH1L2 knockdown and control cells were incubated with sorafenib (5  $\mu\text{M}$ ). Cell proliferation was evaluated using a CCK8 assay (B), a colony formation assay (C), and an EdU incorporation assay (D). ROS levels (E) and apoptosis (F) were evaluated by flow cytometry. (G) The effect of ALDH1L2 overexpression on the IC50 of sorafenib in Huh7 cells was evaluated. (H, I) ALDH1L2-overexpressing and control cells were incubated with sorafenib (5  $\mu\text{M}$ ). Cell proliferation was

that targets Raf-1 and B-Raf and exhibits kinase activity toward proteins in the Ras/Raf/MEK/ERK signaling pathway, platelet-derived growth factor receptor, vascular endothelial growth factor receptor 2, hepatocyte factor receptor (c-KIT), and other proteins to inhibit tumor angiogenesis.<sup>32</sup> However, acquired or intrinsic resistance of cancer cells to sorafenib remains a major obstacle to improving the prognosis of patients with HCC.<sup>32</sup> Epigenetic factors, drug metabolism, dysregulation of apoptosis and characteristics of the tumor microenvironment are the main mechanisms involved in the initiation and development of sorafenib resistance in HCC.<sup>33,47</sup> Therefore, we next investigated whether the knockdown of ALDH1L2 sensitizes HCC cells to sorafenib. When ALDH1L2 expression was silenced by shRNA transduction, Li7 and SNU387 cells exhibited increased sorafenib sensitivity. The IC50 values of sorafenib in Li7/shALDH1L2-1 cells (7.05  $\mu$ M) and Li7/shALDH1L2-2 cells (7.41  $\mu$ M) were lower than those in Li7/shNC (14.23  $\mu$ M) cells. In addition, the IC50 values of sorafenib in SNU387/shALDH1L2-1 cells (8.21  $\mu$ M) and Li7/shALDH1L2-2 cells (8.58  $\mu$ M) were lower than those in SNU387/shNC (13.65  $\mu$ M) cells (Fig. 7A). ALDH1L2 knockdown synergized with sorafenib to suppress the growth of HCC cells and promote ROS release and apoptosis (Fig. 7B–F, Fig. S27A–D). Conversely, ALDH1L2 overexpression significantly decreased the sorafenib sensitivity of Huh7 cells (from 10.31 to 17.59  $\mu$ M) and MHCC-97H cells (from 10.59 to 16.57  $\mu$ M) (Fig. 7G). ALDH1L2 overexpression effectively reversed the promoting effects of sorafenib on cell proliferation inhibition and apoptosis (Fig. 7H and I).

Furthermore, ALDH1L2 knockdown increased the sensitivity of HCC cells to sorafenib *in vivo* in xenograft models. ALDH1L2 knockdown combined with sorafenib treatment reduced the overall tumor volume and mass (Fig. 7J–L). In addition, Ki67 expression was more significantly decreased in the combination group than in the ALDH1L2-knockdown group or the group treated with sorafenib alone (Fig. 7M). These results indicate that the knockdown of ALDH1L2 sensitizes HCC cells to the TKI sorafenib.

## Discussion

Modulation of oxidative stress is currently recognized as an effective approach for anticancer therapy. NRF2 is a basic leucine zipper transcription factor that plays a pivotal role in maintaining redox homeostasis.<sup>34</sup> ROS production in response to oxidative stress is regulated by NRF2.<sup>35</sup> A large body of evidence shows that NRF2 activation in cancer cells promotes cancer progression and metastasis.<sup>36–38</sup> In this study, we found that ALDH1L2 suppresses ROS generation via NRF2 activity. Knockdown of ALDH1L2 inhibits NRF2 expression via the

ubiquitin–proteasome pathway in HCC cells. In addition, we found that NRF2 directly binds to the ALDH1L2 promoter and induces ALDH1L2 expression in HCC cells. Taken together, our results reveal that ALDH1L2 and NRF2 are involved in a positive feedback loop that enables them to maintain cellular redox homeostasis and facilitate HCC cell proliferation and metastasis.

Previous studies have shown that NRF2 binds to the IL-6 gene and activates its expression in hepatic cells.<sup>27</sup> Elevated levels of IL-6 are observed in many solid tumors, including HCC.<sup>39</sup> IL-6 is produced by multiple cell types within the tumor microenvironment, including tumor cells, tumor-infiltrating immune cells and stromal cells.<sup>40</sup> IL-6 acts directly on tumor cells to induce STAT3 expression, which promotes angiogenesis, metastasis, immunosuppression, and accelerates tumor progression.<sup>40</sup> In this study, the plasma IL-6 level was found to be increased in ALDH1L2-overexpressing syngeneic Hepa1-6 model mice. Furthermore, we found that ALDH1L2 activated the Jak2/STAT3 pathway in HCC cells. Pharmacological inhibition and knockdown of STAT3 attenuate ALDH1L2-mediated cell proliferation and invasion in HCC cells. In addition, previous studies have shown that the ability of STAT3 to promote IL-6 gene expression results in a feedforward autocrine feedback loop.<sup>41</sup> Therefore, targeting the ALDH1L2/NRF2 axis is a promising therapeutic approach for treating HCC.

Cancer cell-derived cytokines, such as IL-6, IL-1 $\beta$ , and IL-10, frequently direct differentiating tumor-infiltrating immune cells toward a tumor-promoting phenotype.<sup>42</sup> Previous studies have shown that IL-1 $\beta$  promotes TAM and MDSC infiltration to promote HCC metastasis.<sup>43</sup> Increased infiltration of TAMs has been associated with poor prognosis in HCC.<sup>43,44</sup> TAMs expressing IL-10 have been found to facilitate immune evasion.<sup>45</sup> IL-10 is involved in STAT3 activation, which can contribute to tumor formation. In this study, we found that ALDH1L2 stimulates IL-6 and IL-10 secretion from HCC cells. NF- $\kappa$ B is considered a central mediator of immune and inflammatory responses.<sup>46</sup> Our results show that an increase in the tumor expression level of ALDH1L2, which activates NF- $\kappa$ B signaling in TAMs to generate an inflammatory microenvironment, promotes malignant progression. Furthermore, increased CD206 and CD163 expression was observed in macrophages cocultured with ALDH1L2-overexpressing HCC cells. In addition, CD206-positive M2 macrophages were more abundant in tumors derived from ALDH1L2-overexpressing cells but less abundant in tumors derived from shALDH1L2-transduced cells than in tumors derived from the corresponding control cells. These results indicate that ALDH1L2 promotes the M2 polarization of TAMs, which accelerates HCC progression.

← evaluated by an EdU incorporation assay (H). Apoptosis was evaluated by flow cytometry (I). (J–M) Li7 cells stably expressing shNC or shALDH1L2 were injected subcutaneously into the flanks of nude mice, and the mice were treated with or without sorafenib (10 mg/kg). Tumor growth was measured every 3 days (J). Representative images of excised tumors are shown (K). The tumors were weighed, and the weights were plotted (L). The expression of Ki67 in xenograft tissues was evaluated by IHC staining (M). (N) Model of the mechanisms of action of ALDH1L2 in HCC (figure created with Biorender.com). Data are represented as mean  $\pm$  SD. \**p* <0.05; \*\**p* <0.01. One-way ANOVA. CCK8, Cell Counting Kit-8; HCC, hepatocellular carcinoma; ROS, reactive oxygen species.

In conclusion, we demonstrated that NRF2-induced ALDH1L2 overexpression promotes HCC progression through an IL-6/Jak/STAT3 positive feedback loop, which results in persistent

crosstalk between HCC cells and TAMs and accelerates HCC progression (Fig. 7N). Interference with this oncogenic loop may have great potential therapeutic application in HCC.

## Affiliations

<sup>1</sup>State Key Laboratory of Systems Medicine for Cancer, Shanghai Cancer Institute, Renji Hospital, Shanghai Jiao Tong University School of Medicine, Shanghai, China; <sup>2</sup>Department of Pathology, The Affiliated Hospital of Youjiang Medical University for Nationalities, Baise, Guangxi, China; <sup>3</sup>The Key Laboratory of Molecular Pathology in Tumors of Guangxi Higher Education Institutes, Baise, China; <sup>4</sup>Department of Laboratory Medicine, Jiading Branch of Shanghai General Hospital, Shanghai Jiao Tong University School of Medicine, Shanghai, China; <sup>5</sup>Department of Pathology, Zhongshan Hospital, Fudan University, Shanghai, China

## Abbreviations

AREs, antioxidant response elements; CCK8, Cell Counting Kit-8; ChIP, chromatin immunoprecipitation; DFS, disease-free survival; GEO, Gene Expression Omnibus; HCC, hepatocellular carcinoma; IHC, immunohistochemistry; KEAP1, Kelch-like ECH-associated protein 1; KEGG, Kyoto Encyclopedia of Genes and Genome; MDSC, myeloid-derived suppressor cells; MMPs, matrix metalloproteinases; NF- $\kappa$ B, nuclear factor-kappa B; NRF2, nuclear factor E2-related factor 2; OCR, oxygen consumption rate; OS, overall survival; PHGDH, phosphoglycerate dehydrogenase; qRT-PCR, quantitative real-time-PCR; ROS, reactive oxygen species; SFN, sulforaphane; STAT3, signal transducer and activator of transcription 3; TAMs, tumor-associated macrophages; TCGA, The Cancer Genome Atlas; TKI, tyrosine kinase inhibitor; Treg cell, regulatory T cell; WB, Western blotting; ICGC-LIRI-JP, International Cancer Genome Consortium liver cancer-RIKEN Japan.

## Financial support

This work was supported by grants from the National Natural Science Foundation of China (82273102, 81972581, 82103201, 82300165, 82072892), Shanghai Sailing Program (21YF1445400), State Key Laboratory of Systems Medicine for Cancer Research Foundation (ZZ-94-2312), Guangxi Natural Science Foundation (2024GXNSFAA010061, 2023GXNSFAA026276), the Key Discipline Construction Project of Jiading District Health System (No. XK202405), Guangxi Training Program for Medical High-level Academic Leaders (No. Guiweikejiaofa [2020]-15), Bose Talent Highland (No. 2020-3-2), Building Projects of Guangxi Bagui Scholars (No. 2024), Building Projects from the Key Laboratory of Molecular Pathology (for Hepatobiliary Diseases) of Guangxi (No. Guiweikejiaofa [2020]-17).

## Conflicts of interest

The authors declare no conflict of interest.

Please refer to the accompanying ICMJE disclosure forms for further details.

## Authors' contributions

Designed and supervised research, designed and performed experiments, analyzed data, and wrote the manuscript: HT. Performed experiments: JLL, CZ, QQZ, JYC, QQL, LLM, WT, YY, CG, YTS. Provided technical assistance: JW, XDL.

## Data availability statement

All data are available from the corresponding authors upon reasonable request. RNA-seq data of tumor and non-tumor tissues were obtained from The Cancer Genome Atlas (TCGA; <http://cancergenome.nih.gov>), GEO (GSE22058, GSE67680), and ICGC-LIRI-JP (<https://dcc.icgc.org/projects/LIRI-JP>).

## Supplementary data

Supplementary data to this article can be found online at <https://doi.org/10.1016/j.jhepr.2024.101217>.

## References

Author names in bold designate shared co-first authorship

- [1] Sung H, Ferlay J, Siegel RL, et al. Global Cancer Statistics 2020: GLOBOCAN estimates of incidence and mortality worldwide for 36 cancers in 185 countries. *CA Cancer J Clin* 2021;71:209–249.
- [2] Zhao LN, Bjorklund M, Caldez MJ, et al. Therapeutic targeting of the mitochondrial one-carbon pathway: perspectives, pitfalls, and potential. *Oncogene* 2021;40:2339–2354.
- [3] Ducker GS, Rabinowitz JD. One-carbon metabolism in health and disease. *Cell Metab* 2017;25:27–42.
- [4] Gonen N, Assaraf YG. Antifolates in cancer therapy: structure, activity and mechanisms of drug resistance. *Drug Resist Updat* 2012;15:183–210.
- [5] Schilsky RL. Methotrexate: an effective agent for treating cancer and building careers. The polyglutamate era. *Stem Cells* 1996;14:29–32.
- [6] Yang X, Wang Z, Li X, et al. SHMT2 desuccinylation by SIRT5 drives cancer cell proliferation. *Cancer Res* 2018;78:372–386.
- [7] Pacold ME, Brimacombe KR, Chan SH, et al. A PHGDH inhibitor reveals coordination of serine synthesis and one-carbon unit fate. *Nat Chem Biol* 2016;12:452–458.
- [8] Rossi M, Altea-Manzano P, Demicco M, et al. PHGDH heterogeneity potentiates cancer cell dissemination and metastasis. *Nature* 2022;605:747–753.
- [9] Samanta D, Park Y, Andrabi SA, et al. PHGDH expression is required for mitochondrial redox homeostasis, breast cancer stem cell maintenance, and lung metastasis. *Cancer Res* 2016;76:4430–4442.
- [10] Wei L, Lee D, Law CT, et al. Genome-wide CRISPR/Cas9 library screening identified PHGDH as a critical driver for sorafenib resistance in HCC. *Nat Commun* 2019;10:4681.
- [11] Lee D, Xu IM, Chiu DK, et al. Folate cycle enzyme MTHFD1L confers metabolic advantages in hepatocellular carcinoma. *J Clin Invest* 2017;127:1856–1872.
- [12] Green NH, Galvan DL, Badal SS, et al. MTHFD2 links RNA methylation to metabolic reprogramming in renal cell carcinoma. *Oncogene* 2019;38:6211–6225.
- [13] Krupenko NI, Dubard ME, Strickland KC, et al. ALDH1L2 is the mitochondrial homolog of 10-formyltetrahydrofolate dehydrogenase. *J Biol Chem* 2010;285:23056–23063.
- [14] Strickland KC, Krupenko NI, Dubard ME, et al. Enzymatic properties of ALDH1L2, a mitochondrial 10-formyltetrahydrofolate dehydrogenase. *Chem Biol Interact* 2011;191:129–136.
- [15] Oleinik NV, Krupenko NI, Krupenko SA. ALDH1L1 inhibits cell motility via dephosphorylation of cofilin by PP1 and PP2A. *Oncogene* 2010;29:6233–6244.
- [16] Chen XQ, He JR, Wang HY. Decreased expression of ALDH1L1 is associated with a poor prognosis in hepatocellular carcinoma. *Med Oncol* 2012;29:1843–1849.
- [17] Krupenko NI, Sharma J, Fogle HM, et al. Knockout of putative tumor suppressor Aldh1l1 in mice reprograms metabolism to accelerate growth of tumors in a diethylnitrosamine (DEN) model of liver carcinogenesis. *Cancers (Basel)* 2021;13:3219.
- [18] Noguchi K, Konno M, Koseki J, et al. The mitochondrial one-carbon metabolic pathway is associated with patient survival in pancreatic cancer. *Oncol Lett* 2018;16:1827–1834.
- [19] Miyo M, Konno M, Colvin H, et al. The importance of mitochondrial folate enzymes in human colorectal cancer. *Oncol Rep* 2017;37:417–425.
- [20] Yu L, Guo Q, Luo Z, et al. TXN inhibitor impedes radioresistance of colorectal cancer cells with decreased ALDH1L2 expression via TXN/NF-kappaB signaling pathway. *Br J Cancer* 2022;127:637–648.
- [21] Piskounova E, Agathocleous M, Murphy MM, et al. Oxidative stress inhibits distant metastasis by human melanoma cells. *Nature* 2015;527:186–191.
- [22] Hennequart M, Pilley SE, Labuschagne CF, et al. ALDH1L2 regulation of formate, formyl-methionine, and ROS controls cancer cell migration and metastasis. *Cell Rep* 2023;42:112562.
- [23] LeBleu VS, O'Connell JT, Gonzalez Herrera KN, et al. PGC-1 $\alpha$  mediates mitochondrial biogenesis and oxidative phosphorylation in cancer cells to promote metastasis. *Nat Cell Biol* 2014;16:992–1003. 1001–1015.
- [24] Ju HQ, Lin JF, Tian T, et al. NADPH homeostasis in cancer: functions, mechanisms and therapeutic implications. *Signal Transduct Target Ther* 2020;5:231.

- [25] Harris IS, DeNicola GM. The complex interplay between antioxidants and ROS in cancer. *Trends Cel Biol* 2020;30:440–451.
- [26] Jaramillo MC, Zhang DD. The emerging role of the Nrf2-Keap1 signaling pathway in cancer. *Genes Dev* 2013;27:2179–2191.
- [27] Wruck CJ, Streetz K, Pavic G, et al. Nrf2 induces interleukin-6 (IL-6) expression via an antioxidant response element within the IL-6 promoter. *J Biol Chem* 2011;286:4493–4499.
- [28] Cao Y, Wang J, Tian H, et al. Mitochondrial ROS accumulation inhibiting JAK2/STAT3 pathway is a critical modulator of CYT997-induced autophagy and apoptosis in gastric cancer. *J Exp Clin Cancer Res* 2020;39:119.
- [29] Wang Q, He Z, Huang M, et al. Vascular niche IL-6 induces alternative macrophage activation in glioblastoma through HIF-2alpha. *Nat Commun* 2018;9:559.
- [30] Caetano MS, Zhang H, Cumpian AM, et al. IL6 blockade reprograms the lung tumor microenvironment to limit the development and progression of K-ras-mutant lung cancer. *Cancer Res* 2016;76:3189. 9.
- [31] Saraiva M, Christensen JR, Tsytsykova AV, et al. Identification of a macrophage-specific chromatin signature in the IL-10 locus. *J Immunol* 2005;175:1041–1046.
- [32] Tang W, Chen Z, Zhang W, et al. The mechanisms of sorafenib resistance in hepatocellular carcinoma: theoretical basis and therapeutic aspects. *Signal Transduct Target Ther* 2020;5:87.
- [33] Ladd AD, Duarte S, Sahin I, et al. Mechanisms of drug resistance in HCC. *Hepatology* 2024;79:926–940.
- [34] Rojo de la Vega M, Chapman E, Zhang DD. NRF2 and the hallmarks of cancer. *Cancer Cell* 2018;34:21–43.
- [35] Cloer EW, Goldfarb D, Schrank TP, et al. NRF2 activation in cancer: from DNA to protein. *Cancer Res* 2019;79:889–898.
- [36] Satoh H, Moriguchi T, Takai J, et al. Nrf2 prevents initiation but accelerates progression through the Kras signaling pathway during lung carcinogenesis. *Cancer Res* 2013;73:4158–4168.
- [37] Ngo HKC, Kim DH, Cha YN, et al. Nrf2 mutagenic activation drives hepatocarcinogenesis. *Cancer Res* 2017;77:4797–4808.
- [38] Lignitto L, LeBoeuf SE, Homer H, et al. Nrf2 activation promotes lung cancer metastasis by inhibiting the degradation of Bach1. *Cell* 2019;178:316–329.e318.
- [39] Wong VW, Yu J, Cheng AS, et al. High serum interleukin-6 level predicts future hepatocellular carcinoma development in patients with chronic hepatitis B. *Int J Cancer* 2009;124:2766–2770.
- [40] Johnson DE, O'Keefe RA, Grandis JR. Targeting the IL-6/JAK/STAT3 signalling axis in cancer. *Nat Rev Clin Oncol* 2018;15:234–248.
- [41] Chang Q, Boumazou E, Sansone P, et al. The IL-6/JAK/Stat3 feed-forward loop drives tumorigenesis and metastasis. *Neoplasia* 2013;15:848–862.
- [42] Wang H, Yung MMH, Ngan HYS, et al. The impact of the tumor microenvironment on macrophage polarization in cancer metastatic progression. *Int J Mol Sci* 2021;22:6560.
- [43] He Q, Liu M, Huang W, et al. IL-1beta-Induced elevation of solute carrier family 7 member 11 promotes hepatocellular carcinoma metastasis through up-regulating programmed death ligand 1 and colony-stimulating factor 1. *Hepatology* 2021;74:3174–3193.
- [44] Li Z, Wu T, Zheng B, et al. Individualized precision treatment: targeting TAM in HCC. *Cancer Lett* 2019;458:86–91.
- [45] Wang H, Wang X, Zhang X, et al. The promising role of tumor-associated macrophages in the treatment of cancer. *Drug Resist Updat* 2024;73:101041.
- [46] Taniguchi K, Karin M. NF-kappaB, inflammation, immunity and cancer: coming of age. *Nat Rev Immunol* 2018;18:309–324.
- [47] Yang H, Kang B, Ha Y, et al. High serum IL-6 correlates with reduced clinical benefit of atezolizumab and bevacizumab in unresectable hepatocellular carcinoma. *JHEP Rep* 2023;5:100672.
- [48] Su Y, Meng L, Ge C, et al. PSMD9 promotes the malignant progression of hepatocellular carcinoma by interacting with c-Cbl to activate EGFR signaling and recycling. *J Exp Clin Cancer Res* 2024;43:142.
- [49] Yang X, Yang C, Zhang S, et al. Precision treatment in advanced hepatocellular carcinoma. *Cancer Cell* 2024;42:180–197.

Keywords: ALDH1L2; Feedback loop; TAM; Crosstalk; Progression; Hepatocellular carcinoma.

Received 17 December 2023; received in revised form 2 September 2024; accepted 4 September 2024; Available online 12 September 2024